Journal of Ceramic Processing Research. Vol. 17, No. 6, pp. 537~542 (2016)

J O U R N A L O F
Ceramic Processing Research

Bridgman growth, luminescence and energy transfer studies of Tm^{3+} or/and Dy^{3+} co-doped $Bi_4Si_3O_{12}$ crystal phosphor

Bobo Yang[a,b], Jiayue Xu[a,*], Jun Zou[b], Yan Zhang[a], Tian Tian[a], Yaoqing Chu[a] and Meiling Wang[a]

[a]*Institute of Crystal Growth, School of Materials Science and Engineering, Shanghai Institute of Technology, Shanghai 201418, P.R. China*
[b]*School of Science, Shanghai Institute of Technology, Shanghai 201418, P.R. China*

Tm^{3+}, Dy^{3+} and Tm^{3+}/Dy^{3+} co-doped bismuth silicate ($Bi_4Si_3O_{12}$, BSO) crystals were successfully grown by the modified vertical Bridgeman method. The crystals have about 80% transmittance in the range from 320 nm to 650 nm except several obvious characteristic absorption peaks corresponding to transitions of 4f electrons of Tm^{3+} and Dy^{3+}. The luminescence properties for white light emitting diode (w-LED) were investigated. Energy transfer from the Bi^{3+} ions to the Tm^{3+} and Dy^{3+} ions in Tm^{3+} or/and Dy^{3+} co-doped $Bi_4Si_3O_{12}$ crystal has been established by photoluminescence investigation upon UV excitation. When excited by a proper UV-light, Tm^{3+} doped BSO crystal shows blue emission band centered at 460 nm ascribed to Tm^{3+} ($^1D_2 \rightarrow {}^3F_4$), Dy^{3+} doped BSO crystal shows blue band at 480 nm ($^4F_{9/2} \rightarrow {}^6H_{15/2}$), yellow band at 574 nm ($^4F_{9/2} \rightarrow {}^6H_{13/2}$) and red band at 662 nm ($^4F_{9/2} \rightarrow {}^6H_{11/2}$) of Dy^{3+} ions. A white light with chromaticity coordinate of x = 0.3298, y = 0.2905 by excitation of 357 nm is achieved from Tm^{3+}/Dy^{3+} co-doped $Bi_4Si_3O_{12}$ crystal. These results indicate that Tm^{3+}/Dy^{3+} co-doped $Bi_4Si_3O_{12}$ as a white emitting crystal has a potential application in white-LED.

Key words: Crystal growth, Tm^{3+}/Dy^{3+}:$Bi_4Si_3O_{12}$, Photoluminescence, Energy transfer, White-LED.

Introduction

White light emitting diode (w-LED) is considered to be the next generation solid-state light source that will replace the conventional incandescent and fluorescent lamps because of its high luminous efficiency, long lifetime, great energy saving and environmental safety [1-2]. There are two primary ways of producing white light emitting diodes. One is to use individual LEDs that emit three primary colors-red, green, and blue - and then mix all the colors to form white light [3]. The other is to use a phosphor material to convert monochromatic light from a blue or UV LED to broad-spectrum white lights, much in the same way a fluorescent light bulb works [4-5]. At present, the common way for assemble w-LEDs is combining an ultraviolet (UV) or blue chip with down-converted phosphors [6-7]. Up to now, many studies have been carried out to obtain enough brightness for general lighting, in which useful method is to increase output power of LED chips. However, this also increases the chip temperature, which may cause a deterioration of the resin, which is used to fix the powder phosphors onto the LED chip, and decrease the luminous efficiency and lifetime [8-9]. Compared with powder phosphors, single crystals exhibit good anti-light irradiation, as well as good thermal, mechanical, and chemical stability. The rigid cyclic symmetric structure of single crystals results in the high luminous efficiency of active ions. These excellent properties of single crystals are beneficial for LED applications to obtain high stability, long lifetime, high luminous efficiency, and good white color. Thus, it is a promising way to use single crystals as phosphor in LED application [10-11].

Bismuth silicate ($Bi_4Si_3O_{12}$, BSO) crystal is known as an excellent scintillator, and has attracted broad interest in high-energy and nuclear physics experiments [12-14]. It has excellent properties, such as high hardness, large specific heat, small thermal expansion, high optical damage threshold, and high optical transmittance, which render it as a latent phosphor host material for LED application. However, it is difficult to grow BSO crystal due to the compositional deviation in the melt [15-16]. Several methods were used to grow BSO crystals, such as Czochralski [17] and Bridgman [15-16, 18-19] growth method. Among these methods, the vertical Bridgeman method was proved to be a successful way to grow large and high quality BSO crystals. In previous work, we have reported the growth and scintillation properties of pure and rare earth doped BSO crystals [20-23]. The cost of growing BSO crystals is much lower than growing YAG crystals or other crystals for LED as the lower cost of feed materials and lower melting point. It was reported that Dy^{3+}: BSO powder was a kind of direct white light phosphor under UV excitation [24]. However, our recent research revealed Dy^{3+}: BSO crystal as a yellow

*Corresponding author:
Tel : +86-021-60873581
E-mail: xujiayue@sit.edu.cn

emitting phosphor, not a white light phosphor.[25] The visible luminescence of Dy^{3+} ($^4f_9$) ion mainly consists of two intense bands in the blue (470 nm ~ 500 nm) and yellow (570 nm ~ 600 nm) regions, which are associated with the $^4F_{9/2}$-$^6H_{15/2}$ and $^4F_{9/2}$-$^6H_{13/2}$ transitions, respectively. The latter one is a hypersensitive transition, which is strongly influenced by the environment [26-28]. For BSO:Dy^{3+} crystal, the intensity of yellow emissions is much stronger than that of blue emissions, so the mixed colors then form just stable yellow light. In order to obtain white light, it may be a feasible way to dope Dy^{3+} ions with other RE ions in BSO. Tm^{3+} always can act as a blue luminescence center in many host materials [29-30]. Thus, introducing the Tm^{3+} into the Dy^{3+}-activated system may lead the generation of white light. To the best of our knowledge, the investigation of Dy^{3+}-Tm^{3+} co-doped $Bi_4Si_3O_{12}$ crystal has not yet been reported until now. In this paper, we report the growth of Tm^{3+} or/and Dy^{3+} co-doped $Bi_4Si_3O_{12}$ single crystal by Bridgman method and demonstrate the capability of generating white light under excitation at UV light.

Experimental

Crystal growth

High purity Tm_2O_3 (> 4N), Dy_2O_3 (> 4N), SiO_2 (> 4N) and Bi_2O_3 (> 5N) were used as starting materials for Tm or/and Dy co-doped BSO single crystal growth. These starting materials were weighed according to the formula of $(Bi_{0.995}Tm_{0.005})_4Si_3O_{12}$, $(Bi_{0.99}Dy_{0.01})_4Si_3O_{12}$ and $(Bi_{0.985}Tm_{0.005}Dy_{0.01})_4Si_3O_{12}$ and mixed in a ball mill coated with polyethylene for 8h. The mixture was then held at 750°Ê for 10hrs. After sintering, it was ground to powders and mixed again in the ball mill for 3hrs. The samples were then put into the aluminum oxide crucible and held at 850 ºC for 12hrs to prepare Tm^{3+} or/and Dy^{3+} co-doped $Bi_4Si_3O_{12}$ polycrystalline powders. The polycrystalline feed materials were then loaded into the Pt crucible to grow single crystal in the Bridgman furnace. The Pt crucible was designed with a seed well. In this work, the orientation of the seed crystal was chosen to be <001>. The furnace temperature was set to 50 ºC higher than the melting point of BSO (1025 ºC) and controlled by an automatic temperature controller with an accuracy of ±2 ºC. The charge was kept at high temperature for several hours to ensure complete melting and to provide a stable temperature distribution. Then the crucible system was cooled at a rate of 0.2 ~ 0.5 mm/h to room temperature, and the crystals were taken out by tearing the crucible. Tm^{3+} or/and Dy^{3+}co-doped $Bi_4Si_3O_{12}$ crystals with a size of about ϕ25 mm × 80 mm were successfully grown one time by the modified vertical Bridgeman method.

Characterization

The as grown crystals were cut and polished for measurement. Powder X-ray diffraction (XRD) was performed to examine the phase structure of the as-grown crystal using a D/max-2200 PC type diffractometer (Rigaku Co. Ltd., Tokyo, Japan) at room temperature. Polished square doped BSO crystal pieces with a width of 8mm and a thickness of 2 mm were prepared. Transmittance spectra were measured by means of a spectrophotometer (Model Cary 5000 UV-VIS-NIR) at room temperature in the wavelength range of 250 nm ~ 650 nm. The room temperature excitation, fluorescence spectra and decay curves were carried out with Edinburgh Instruments FLS920 spectrophotometer, using Xenon lamp as a light source.

Results and Discussion

The XRD pattern of the Tm^{3+}/Dy^{3+} co-doped BSO sample is shown in Fig. 1. Based on the PDF#33-0215, the XRD spectrum shows that the diffraction peaks and relative intensity of the crystal sample are in agreement with the formation of orthorhombic structured BSO. No impurity phase such as the Tm_2O_3 and Dy_2O_3 was detected in the doped sample. A small shift of the diffraction peaks is attributed to the lattice distortion resulted from the accommodation of Tm^{3+} and Dy^{3+}in the $Bi_4Si_3O_{12}$ lattices. The Lattice constants of the as-grown Tm^{3+}/Dy^{3+} co-doped $Bi_4Si_3O_{12}$ crystal are a = b = c = 1.0282 nm calculated from the XRD patterns.

The transmittance spectra of Tm^{3+} or/and Dy^{3+} co-doped $Bi_4Si_3O_{12}$ crystal samples is shown in Fig. 2. The crystals have about 80% transmittance in the range from 320 nm to 650 nm. For Tm^{3+}:$Bi_4Si_3O_{12}$ crystal sample, there is one absorption band are observed at 357 nm in the UV region. For Dy^{3+}:$Bi_4Si_3O_{12}$ crystal sample, there are several obvious characteristic absorption bands corresponding to transitions of 4f electrons of Dy^{3+} at 323 nm, 348 nm, 363 nm, 390 nm in the UV region. For Tm^{3+}/Dy^{3+} co-doped $Bi_4Si_3O_{12}$ crystal sample, there are several obvious characteristic absorption bands corresponding to transitions of 4f

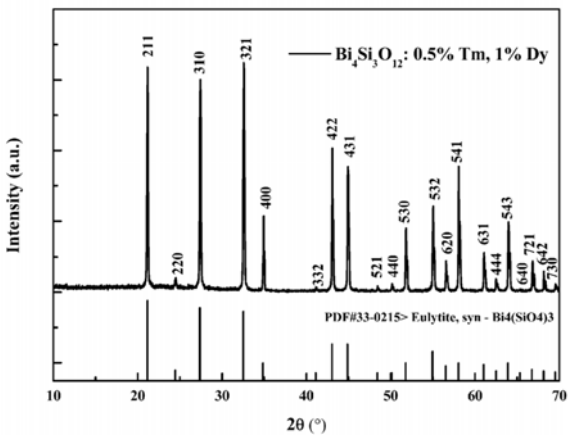

Fig. 1. Powder X-ray diffraction patterns of the Tm^{3+}/Dy^{3+} co-doped BSO crystal.

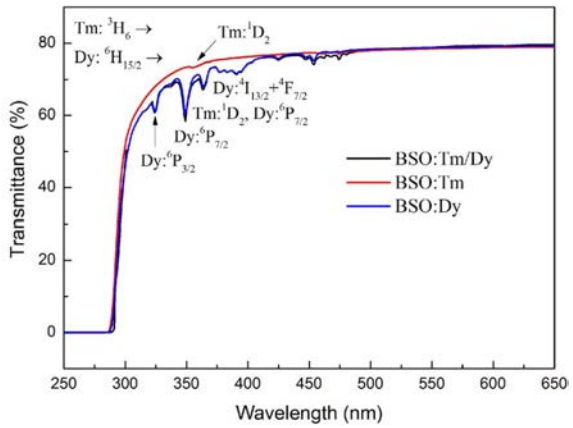

Fig. 2. Transmittance spectra of Tm^{3+} or/and Dy^{3+} co-doped $Bi_4Si_3O_{12}$ crystal sample.

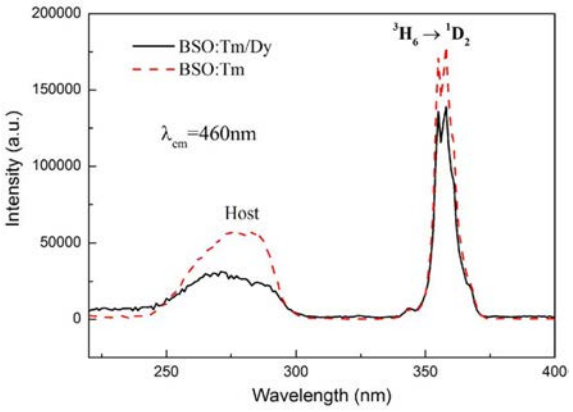

Fig. 3. Excitation spectra of Tm^{3+} and Tm^{3+}/Dy^{3+} co-doped $Bi_4Si_3O_{12}$ crystal monitored at 460 wavelengths.

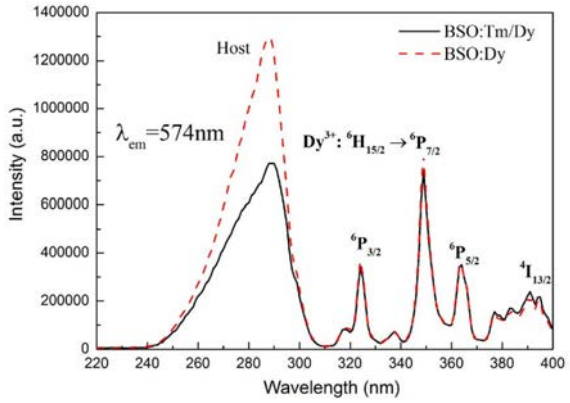

Fig. 4. Excitation spectra of Dy $^{3+}$ and Tm^{3+}/Dy^{3+} co-doped $Bi_4Si_3O_{12}$ crystal monitored at 574 wavelengths.

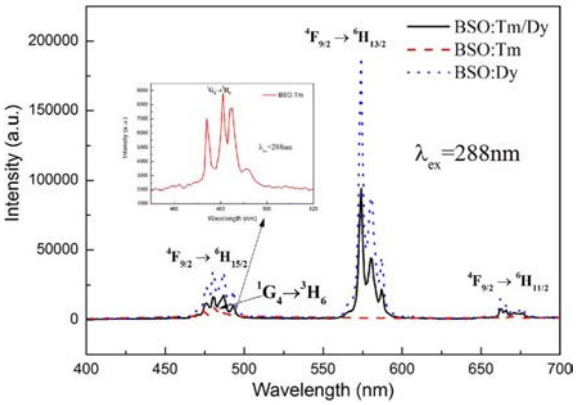

Fig. 5. Emission spectra of Tm^{3+} or/and Dy^{3+} co-doped $Bi_4Si_3O_{12}$ crystals under excited by 288 nm.

electrons of Tm^{3+} and Dy^{3+} at 323 nm, 348 nm, 357 nm, 363 nm, 390 nm in the UV region of the transmission curves. All the absorption bands can be ascribed to the transitions from the ground states of Tm^{3+}/Dy^{3+} to their excited states which are labeled, respectively. It seems that the optical absorption strength of Tm^{3+}/Dy^{3+}co-doped $Bi_4Si_3O_{12}$ crystal is the superposition of the Tm^{3+} and Dy^{3+} single doped $Bi_4Si_3O_{12}$ crystal.

Fig. 3 shows excitation spectra of Tm^{3+} and Tm^{3+}/Dy^{3+} co-doped $Bi_4Si_3O_{12}$ crystal samples at room temperature monitored at 460 nm wavelengths. From Fig. 3, we can find that for the both two crystals there is a broad band in a wavelength range between about 240 nm and 310 nm corresponding to oxygen to bismuth charge transfer band, and one excitation peak located at about 357 nm band corresponding to the transitions of $^3H_6 \rightarrow {}^1D_2$ of Tm^{3+}, in the excitation spectrum monitored at 460 nm. The excitation spectra showed an overlap between 220 nm and 400 nm, which indicates that the emission at 460 nm is just ascribed to Tm^{3+} in Tm^{3+}/Dy^{3+} co-doped $Bi_4Si_3O_{12}$ crystal. It is observed that the excitation spectrum monitored at 574 nm of Tm^{3+}/Dy^{3+} co-doped $Bi_4Si_3O_{12}$ crystal sample from Fig. 4 consists of a broad band in a wavelength range between about 240 nm and 310 nm corresponding to oxygen to bismuth charge transfer band. Above about 288 nm, which corresponds to the band gap of BSO, all the excitation peaks can be assigned to the 4f-4f transitions of Dy^{3+}. Like the phenomenon described of the excitation spectra of Tm^{3+} and Tm^{3+}/Dy^{3+} co-doped $Bi_4Si_3O_{12}$ crystal, the excitation spectra showed an overlap between 220 nm and 400 nm in Dy^{3+} and Tm^{3+}/Dy^{3+} co-doped $Bi_4Si_3O_{12}$ crystal, which indicates that the emission at 574 nm is just due to Dy^{3+} in Tm^{3+}/Dy^{3+} co-doped $Bi_4Si_3O_{12}$ crystal.

Fig. 5 shows photoluminescence emission spectra of Tm^{3+} or/and Dy^{3+} co-doped $Bi_4Si_3O_{12}$ crystal samples at room temperature under the excitation of 288 nm. It is clear from Fig. 5 that when excited by 288 nm, the emission spectra of the Dy^{3+} and Tm^{3+}/Dy^{3+} co-doped $Bi_4Si_3O_{12}$ crystals show a blue band at 480 nm ($^4F_{9/2} \rightarrow {}^6H_{15/2}$), a yellow band at 574 nm ($^4F_{9/2} \rightarrow {}^6H_{13/2}$) and a red band at 662 nm ($^4F_{9/2} \rightarrow {}^6H_{11/2}$) of Dy^{3+}, while the emission spectra of Tm^{3+} doped $Bi_4Si_3O_{12}$ crystal show only one blue band at 480 nm ($^1G_4 \rightarrow {}^3H_6$) of Tm^{3+}.

According to the excitation and emission spectra of these crystal samples, it can be concluded that for Tm^{3+} or Dy^{3+} single doped $Bi_4Si_3O_{12}$ crystal, the energy absorbed by Bi atoms then is transferred to Tm or Dy.

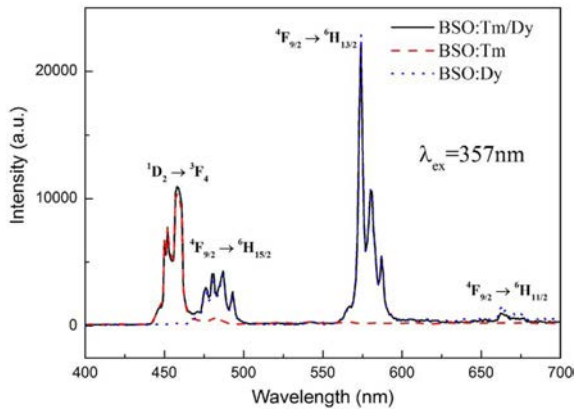

Fig. 6. Emission spectra of Tm^{3+} or/and Dy^{3+} co-doped $Bi_4Si_3O_{12}$ crystals under excited by 357 nm.

While for Tm^{3+} and Dy^{3+} co-doped $Bi_4Si_3O_{12}$ crystal, the energy absorbed by Bi atoms then is largely transferred to only Dy.

Photoluminescence emission spectra of Tm^{3+} or/and Dy^{3+} co-doped $Bi_4Si_3O_{12}$ crystal samples at room temperature under the excitation of 357 nm is shown in Fig. 6. When excited by 357 nm, the emission spectra of the Tm^{3+}/Dy^{3+} co-doped $Bi_4Si_3O_{12}$ crystal show a blue band at 480 nm ($^4F_{9/2} \rightarrow {}^6H_{15/2}$), a yellow band at 574 nm ($^4F_{9/2} \rightarrow {}^6H_{13/2}$) and a red band at 662 nm ($^4F_{9/2} \rightarrow {}^6H_{11/2}$) of Dy^{3+} like the emission spectra of the Dy^{3+} doped $Bi_4Si_3O_{12}$ crystal, as well as a blue band at 460 nm ($^1D_2 \rightarrow {}^3F_4$) of Tm^{3+} like the emission spectra of the Tm^{3+} doped $Bi_4Si_3O_{12}$ crystal. In other word, the emission strength of the Tm^{3+}/Dy^{3+} co-doped $Bi_4Si_3O_{12}$ crystal is the superposition of the Tm^{3+} and Dy^{3+} single doped $Bi_4Si_3O_{12}$ crystal. These results indicated that there is no energy transfer between Tm^{3+} and Dy^{3+}.

Fig. 7 shows the decay curves of Tm^{3+}: $^1D_2$ emission level and Dy^{3+}: $^4F_{9/2}$ in Tm^{3+} or/and Dy^{3+} co-doped $Bi_4Si_3O_{12}$ crystal under 357 nm excitation monitoring the emission at 460 nm ($^1D_2 \rightarrow {}^3F_4$) and 574 nm ($^4F_{9/2} \rightarrow {}^6H_{13/2}$) respectively. From these decay profiles the lifetime has been determined by taking the first e-folding times of the intensity of decay curves. All the decay curves are well fitted to a single exponential function: $I = I_0 e^{-t/\tau}$, where I is the intensity at time t, I_0 is the initial intensity when t = 0 and ô is the lifetime. The lifetime values of $^1D_2$ level in Tm^{3+}/Dy^{3+} co-doped $Bi_4Si_3O_{12}$ and Tm^{3+} single doped $Bi_4Si_3O_{12}$ crystal are found to be 23.08 ìs and 26.71 μs. The lifetime values of $^4F_{9/2}$ level in Tm^{3+}/Dy^{3+} co-doped $Bi_4Si_3O_{12}$ and Dy^{3+} single doped $Bi_4Si_3O_{12}$ crystal are found to be 623.48 μs and 628.33 μs. The decay lifetime for Tm^{3+} or Dy^{3+} was found to decrease with codoping Dy^{3+} or Tm^{3+}, which may originate from the energy transfer mechanism in the Tm^{3+}/Dy^{3+} co-doped $Bi_4Si_3O_{12}$, but it is not simply due to the energy transfer from Tm^{3+} to Dy^{3+} or Dy^{3+} to Tm^{3+}.

The CIE chromaticity coordinates of the Tm^{3+} or/and Dy^{3+} co-doped BSO crystals under 288 nm excitation were calculated using the corresponding emission spectrum in Fig. 5 and were presented in Table 1. Upon excitation at 288 nm, the Dy^{3+} and Tm^{3+}/Dy^{3+} co-doped

Table 1. Chromaticity coordinates of crystal samples under 288 nm excitation.

samples	x-coordinate	y-coordinate
Tm^{3+} : $Bi_4Si_3O_{12}$	0.1864	0.2458
Dy^{3+} : $Bi_4Si_3O_{12}$	0.4153	0.4328
Tm^{3+}/Dy^{3+} : $Bi_4Si_3O_{12}$	0.4146	0.4296

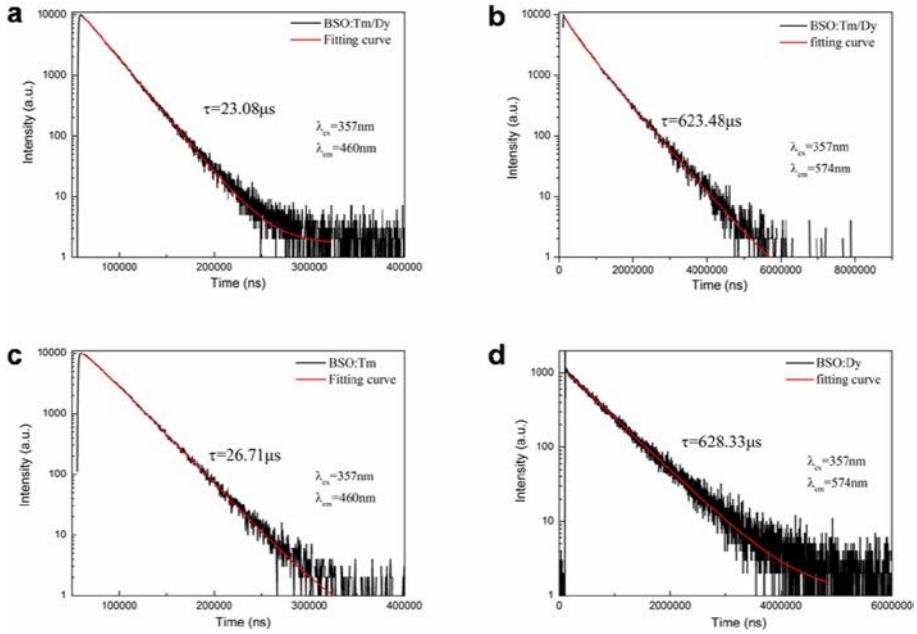

Fig. 7. Photoluminescence decay curves of Tm^{3+} and Dy^{3+} in Tm^{3+} or/and Dy^{3+} co-doped $Bi_4Si_3O_{12}$ crystal under 357 nm excitation monitoring the emission at 460 nm and 574 nm

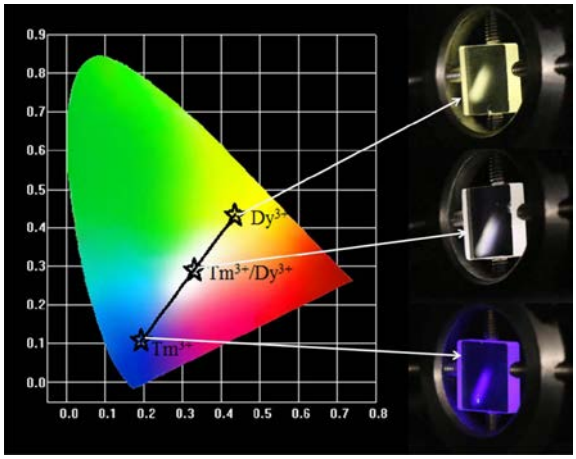

Fig. 8. CIE chromaticity coordinates and the polished sample of the Tm^{3+} or/and Dy^{3+} co-doped BSO crystals under excited by 357 nm.

BSO crystal samples exhibit yellow light, and the Tm^{3+} doped BSO crystal sample exhibit blue light. Fig. 8 illustrates the CIE chromaticity coordinates of the Tm^{3+} or/and Dy^{3+} co-doped BSO crystals under 357 nm excitation which calculated using the corresponding emission spectrum in Fig. 6. From Fig. 8, we can see that upon excitation at 357 nm, the Tm^{3+} and Dy^{3+} single doped BSO crystal emits blue and yellow light respectively while the Tm^{3+} and Dy^{3+} co-doped BSO crystal can emit white light and the CIE coordinate is ($x = 0.3298$, $y = 0.2905$, $Tc = 5598$ K). The color temperature Tc can be obtained from the color temperature calculation software. Therefore, based on the excitation and emission spectra along with the CIE chromaticity coordinates, the emission color of Tm^{3+}/Dy^{3+} co-doped BSO crystal can be tuned from yellow light to white light. In other words, the white light emission can be obtained from the Tm^{3+}/Dy^{3+} co-doped $Bi_4Si_3O_{12}$ crystal excited with proper UV-light.

Conclusions

In summary, Tm^{3+} or/and Dy^{3+} co-doped $Bi_4Si_3O_{12}$ single crystals with good quality and optical properties was grown by Bridgman method. The crystals have about 80% transmittance in the range from 350 nm to 650 nm except several obvious characteristic absorption peaks corresponding to transitions of 4f electrons of Tm^{3+} and Dy^{3+}. The energy transfer from Bi^{3+} to Tm^{3+} and Dy^{3+} has been established by photoluminescence investigation upon UV excitation. There is no energy transfer between Tm^{3+} and Dy^{3+} in Tm^{3+} and Dy^{3+} co-doped $Bi_4Si_3O_{12}$ crystal. The emission color of the crystal was found tunable by varying the excitation wavelength. The calculated chromaticity coordinate is (0.3298, 0.2905) for Tm^{3+} and Dy^{3+} co-doped $Bi_4Si_3O_{12}$ under 357 nm excitation, which lies in the white light area. Therefore, the Tm^{3+} and Dy^{3+} co-doped $Bi_4Si_3O_{12}$ single crystal is a potential phosphor for white LED.

Acknowledgments

This work was supported by the National Science Foundation of China (51342007), the National Key Basic Research Program (2011CB612310), Shanghai Committee of Science and Technology Research Projects (14500 503300), National Science Foundation of China (5130 2171), Shanghai Alliance Program (Lm201318) and Shanghai Cooperative Project (ShanghaiCXY-2013-61).

References

1. E.F. Schubert and J.K. Kim, Science308 (2005) 1274.
2. N. Kimura, K. Sakuma, S. Hirafune, K. Asano, N. Hiroski and R.J. Xie, Appl. Phys. Lett., 90 (2007) 051109.
3. J.H. Wold and A. Valberg, Color Res. Appl. 26[S1] (2000) S222.
4. M. Bessho and K. Shimizu, Electr. Commun. Jpn. 95 (2012) 1-7.
5. Y. Zhou, J.Y. Xu, Z.J. Zhang and M.J. You, J. Alloys Compd. 615 (2014) 624-628.
6. J.K. Sheu, S.J. Chang, C.H. Kuo, Y.K. Su, L.W. Wu, Y.C. Lin, W.C. Lai, J.M. Tsai, G.C. Chi and R.K. Wu, IEEE Photon. Technol. Lett. 15(2003) 18-20.
7. N. Yukio, N. Junya, S. Takahiko, D. Kouichiro, Y. Takao and M. Takashi, Jpn. J. Appl. Phys. 45 (2006) L1084-L1086.
8. E. Malchukova and B. Boizot, J. Rare Earths 32[3] (2014) 217-220.
9. B. Joshi, Y.K. Kshetri, G. Gyawali and S.W. Lee, J. Alloys Compd. 631 (2015) 38-45.
10. L.H.C. Andrade, S.M. Lima, R.V. Silva, M.L. Baesso, Y. Guyot and L.A.O. Nunes, J. Mater. Chem. C[2] (2014) 10149-10156.
11. W.D. Xiang, J.S. Zhong, Y.S. Zhao, B.Y. Zhao, X.J. Liang, Y.J. Dong, Z.M. Zhang, Z.P. Chen and B.F. Liu, J. Alloys Compd. 142 (2012) 218-221.
12. H. Shimizu, F. Miyahara, H. Hariu, T. Hayakawa, T. Ishikawa, M. Itaya, T. Iwata, T. Kinoshita, M. Moriya, T. Nakabayashi, T. Sasaki, Y. Tajima, S. Takita, M. Yamamoto, H. Yamazaki, H.Y. Yoshida and Y. Yoshida, Nucl. Instrum. Methods Phys. Res. A. 550 (2005) 258-266.
13. J.T. He, G.Y. Zhu, D.B. Chen, X.L. Dong, Z.B. Li, J.G. Bian, S.J. Fan, R.Y. Sun, Y.F. Lin, Y.T. Fei and J.Y. Xu, High Energ. Phys. Nucl. Phys. (in Chin.) 21 (1997) 886-890.
14. N. Akchurin, M. Alwarawrah, A. Cardini, G. Ciapetti, R. Ferran, S. Franchino, M. Fraternali, G. Gaudio, J. Hauptman, F. Lacava, L.L. Rotonda, M. Livan, E. Meoni, D. Pinci, A. Policicchio, S. Popescu, G. Susinno, Y. Roh, W. Vandelli, T. Venturelli, C. Voena, I. Volobouev and R. Wigmans, Nucl. Instrum. Methods Phys. Res. A. 598 (2009) 710-721.
15. J.Y. Xu, H. Wang, Q.B. He, H. Shen, H.J. Shimizu and W.D. Xiang, J. Chin. Ceram. Soc. 37 (2009) 295-298.
16. Y.T. Fei, S.J. Fan, R.Y. Sun and M. Ishii, Prog. Cryst. Growth Charact. Mater. 40 (2000) 183-188.
17. H. Jiang, H.J. Kim, G. Rooh, H. Park, S. Kim and J.K. Cheon, Nucl. Instrum. Methods Phys. Res. A. 648 (2011) 73-76.
18. M. Ishii, K. Harada, N. Senguttuvan, M. Kobayashi and I.Yamaga, J. Cryst. Growth 205 (1999) 191-195.
19. M. Ishii, K. Harada, Y. Hirose, N. Senguttuvan, M. Kobayashi, I. Yamaga, H. Ueno, K. Miwa, S.J. Fan, Y.T. Fei, M. Nikl and X.Q. Feng, Opt. Mater. 19 (2002) 201-212.

20. Y. Zhang, J.Y. Xu and B.L. Lu, J. Alloys Compd. 582 (2014) 635-639.
21. Y. Zhang, J.Y. Xu, Q.B. He and B.L. Lu, J. Cryst. Growth 362 (2013) 121-124.
22. Y. Zhang, J.Y. Xu and P.F. Shao, J. Cryst. Growth 318 (2011) 920-923.
23. H. Shen, J.Y. Xu, W.J. Ping, Q.B. He, Y. Zhang, M. Jin and G.J. Jiang, Chin. Phys. Lett. 29 (2012) 076501.
24. Q.H. Wei, G.H. Liu, Z.Z. Zhou, H. Yang, J.D. Zhuang and Q. Liu, J. Lumin. 145 (2014) 803-807.
25. B.B. Yang, J.Y. Xu, Y. Zhang, Y.Q. Chu, M.L. Wang and Y.X. Wen, Mater. Lett. 135 (2014) 176-179.
26. G. Dzik, W. Romanowski, R. Lisiecki, P. Solarz and M. Berkowski, Appl. Phys. B. 99 (2010) 285-297.
27. P. Babu, K.H. Jang, E.S. Kim, L. Shi, H.J. Seo, F. Rivera-López, U.R. Rodríguez-Mendoza, V. Lavín, R. Vijaya, C.K. Jayasankar and Rama L, J. Appl. Phys. 105 (2009) 013516.
28. M. So³tys, L. ¯ur, J. Pisarska and W.A. Pisarski, J. Rare Earths 32[3] (2014) 213-216.
29. L. Tang, H.P. Xia, P.Y. Wang, J.T. Peng, Y.P. Zhang and H.C. Jiang, J. Mater. Sci. 48 (2013) 7518-7522.
30. J.Y. Wang, J.B. Wang and P. Duan, Opt. Mater. 36 (2013) 572-574.